ARTICLE

Incorporation of Graphenes in Nanostructured TiO_2 Films *via* Molecular Grafting for Dye-Sensitized Solar Cell Application

Yong-Bing Tang,[†,‡,§] Chun-Sing Lee,[‡,*] Jun Xu,[‡] Zeng-Tao Liu,[‡] Zhen-Hua Chen,[‡] Zhubing He,[‡] Yu-Lin Cao,[‡] Guodong Yuan,[‡] Haisheng Song,[‡] Limiao Chen,[‡] Linbao Luo,[‡] Hui-Ming Cheng,[§] Wen-Jun Zhang,[‡] Igor Bello,[‡] and Shuit-Tong Lee[†,‡,*]

[†]Institute of Functional Nano & Soft Materials (FUNSOM) and Jiangsu Key Laboratory for Carbon-Based Functional Materials & Devices, Soochow University, Suzhou, Jiangsu 215123, People's Republic of China, [‡]Center of Super-Diamond and Advanced Films (COSDAF) and Department of Physics and Materials Science, City University of Hong Kong, Hong Kong SAR, People's Republic of China, and [§]Shenyang National Laboratory for Materials Science (SYNL), Institute of Metal Research, Chinese Academy of Sciences, Shenyang 110016, People's Republic of China

ABSTRACT This paper presents a systematic investigation on the incorporation of chemical exfoliation graphene sheets (GS) in TiO_2 nanoparticle films *via* a molecular grafting method for dye-sensitized solar cells (DSSCs). By controlling the oxidation time in the chemical exfoliation process, both high conductivity of reduced GS and good attachment of TiO_2 nanoparticles on the GS were achieved. Uniform GS/TiO_2 composite films with large areas on conductive glass were prepared by electrophoretic deposition, and the incorporation of GS significantly improved the conductivity of the TiO_2 nanoparticle film by more than 2 orders of magnitude. Moreover, the power conversion efficiency for DSSC based on GS/TiO_2 composite films is more than 5 times higher than that based on TiO_2 alone, indicating that the incorporation of GS is an efficient means for enhancing the photovoltaic (PV) performance. The better PV performance of GS/TiO_2 DSSC is also attributed to the better dye loading of GS/TiO_2 film than that of TiO_2 film. The effect of GS content on the PV performances was also investigated. It was found that the power conversion efficiency increased first and then decreased with the increasing of GS concentration due to the decrease in the transmittance at high GS content. Further improvements can be expected by fully optimizing fabrication conditions and device configuration, such as increasing dye loading *via* thicker films. The present synthetic strategy is expected to lead to a family of composites with designed properties.

KEYWORDS: graphenes · titanium dioxide · molecular-level incorporation · composite films · dye-sensitized solar cells

*Address correspondence to apcslee@cityu.edu.hk, apannale@cityu.edu.hk.

Received for review March 4, 2010 and accepted May 6, 2010.

Published online May 10, 2010. 10.1021/nn100449w

Graphene, as individual sheets of carbon atoms bonded in a honeycomb lattice, has attracted much attention because of its unique properties and potential applications.[1−3] Charge carriers in graphene sheets (GS) obey a linear dispersion relation near the Fermi energy and behave as massless Dirac fermions,[1−4] resulting in many unusual attributes such as the quantum Hall effect[3,4] and ambipolar electric field effect.[1] Furthermore, GS exhibits nondispersive transport characteristics and extremely high electron mobility (~15 000 $cm^2/(V \cdot s)$) at room temperature.[1−3] Recently, much progress has been achieved in the fabrication of single- or multilayer GS into functional devices such as field-effect transistors,[1,5−9] ultrasensitive sensors,[10] and organic photovoltaic cells.[11] In addition to device applications, graphene also can serve as reinforcement to enhance mechanical, thermal, or electrical properties in composite materials.[12−14] The ease of incorporation of GS into polymers or ceramics offers an effective means for realization of conducting composites from insulating matrix materials.[13,14] A GS volume fraction as low as 0.1 vol % could already dramatically improve electrical conductivity of polymer−matrix composites owing to GS's excellent transport properties, high aspect ratio (the ratio of lateral size to thickness), and large surface area.[12]

The interest in photovoltaic (PV) devices has long been motivated by the need to supplement or even replace fossil fuels with clean and renewable energy resources. Dye-sensitized solar cell (DSSC) is a promising technology for converting sunlight into electrical energy, as it possesses such advantages as low cost, simple process, and large-scale production.[15] The photoanodes of DSSCs are typically constructed using thick films (10−15 μm) of TiO_2 nanoparticles that are processed as a paste and sintered into a mesoporous network.[16,17] The thick nanoparticle film provides a large surface area for anchoring enough dye molecules. However, electron transport in disordered TiO_2 nanoparticles proceeds by a trap-limited diffusion process,[17] in which injected electrons travel through a large num-

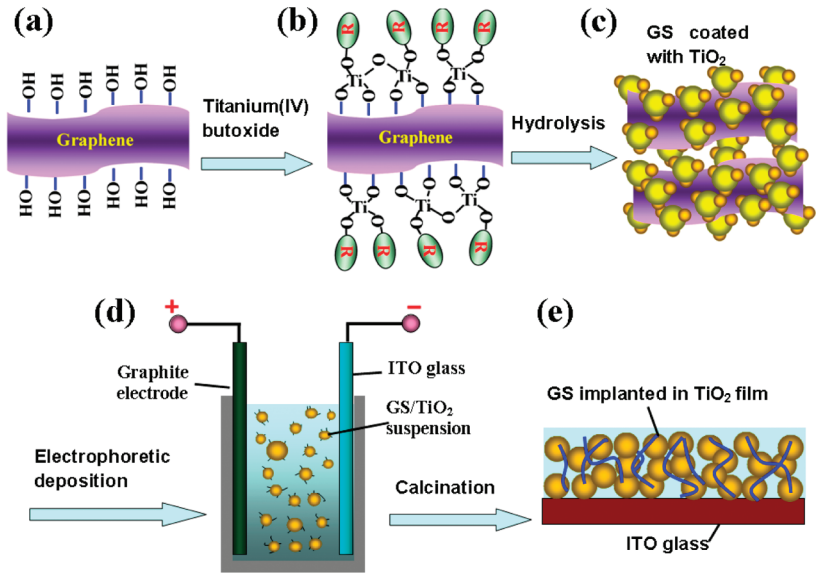

Figure 1. Schematic flowchart of *in situ* incorporation of GS in nanostructured TiO_2 films. (a) GS prepared by chemical exfoliation with residual oxygen-containing functional groups, such as hydroxyl. (b) Schematic of titanium(IV) butoxide grafted on the reduced GS surfaces by chemisorption. (c) Schematic diagram of GS coated with TiO_2 colloids after hydrolysis. (d) Illustration of the electrophoretic deposition process used to prepare GS/TiO_2 composite films. (e) Schematic representation of the structure of the GS/TiO_2 composite film after calcination.

ber of colloidal particles and grain boundaries before reaching the collecting electrode. Such a random transit path for the photogenerated electrons increases the chance of carrier recombination and thus decreases the efficiency of DSSCs.[16,17] It is expected that improving the conduction pathways from the point of photogenerated carriers to the collecting electrode would significantly improve the power conversion efficiency.[18−21] Carbon nanotubes have been incorporated into TiO_2 films to enhance carrier transport in photoelectrochemical solar cells.[20,21] More recently, some research groups have fabricated TiO_2−graphene composites,[22−24] which exhibited excellent photoconversion and photocatalyst properties.[23,24] Here, we report *in situ* incorporation of GS in TiO_2 nanoparticle films by a molecular grafting method for application in DSSCs, as schematically illustrated in Figure 1. The incorporation of graphenes significantly improved the conductivity of the TiO_2 films and the PV performance.

RESULTS AND DISCUSSION

Preparation of Graphenes. To obtain a large quantity of GS and uniform solution dispersion capability for our application, we prepared GS suspension by chemical reduction of exfoliated graphite oxide.[25] In a typical process, graphene oxide (GO) was synthesized by a modified Hummers' method[26] through strong acid oxidation of natural graphite powder, followed by exfoliation in water with the aid of mild sonication (see Experimental Section and Supporting Information). Three GO suspensions were prepared with different oxidation times of 5, 10, and 20 h by the mixture of potassium permanganate and strong acids, and the samples are denoted as 1, 2, and 3, respectively. Then, all suspensions were reduced by hydrazine for the same time and centrifuged to form homogeneous GS dispersions, which were dried *via* evaporation of water. Before reaction with titanium alkoxide precursor, the as-prepared GS were dispersed again in anhydrous ethanol by sonication. The resultant suspensions were stable and homogeneous (Figure 2a, right) due to the presence of residual polar oxygen-containing groups on GS surfaces.[12] Atomic force microscopy (AFM) shows the obtained GS are relatively smooth (Figure S1, Supporting Information), similar to that obtained by micromechanical cleavage.[1−3] Figure 2b shows an AFM image of a monolayer GS from sample 2 with a thickness of ~1.03 nm and a lateral size on the order of micrometers. Approximately 80% of the sheets have heights of 1.0 ± 0.3 nm. Figure 2c presents a typical low-magnification transmission electron microscopy (TEM) image of a GS in sample 2. The corresponding electron diffraction (ED) pattern (Figure 2d) matches well with those observed in mechanically cleaved GS.[10] Morphologies and crystal structures of all other samples were found to be similar to those of sample 2.

Conductivity of the Reduced GS. The effect of oxidation time on the conductivity of the reduced GS was investigated by constructing two-terminal devices based on individual graphene (Supporting Information, Figure S2). To assess the electrical properties with enough statistics, we have fabricated and measured at least 10 devices based on individual GS for each sample. It was found that the conductivity of GS decreased from sample 1 to sample 3. The current response at 1.0 V for sample 1 is in the range of 78−91 μA, whereas the conductivity decreases to 46−59 μA for sample 2 and 16−27 μA for sample 3 (Figure S2d). These results show

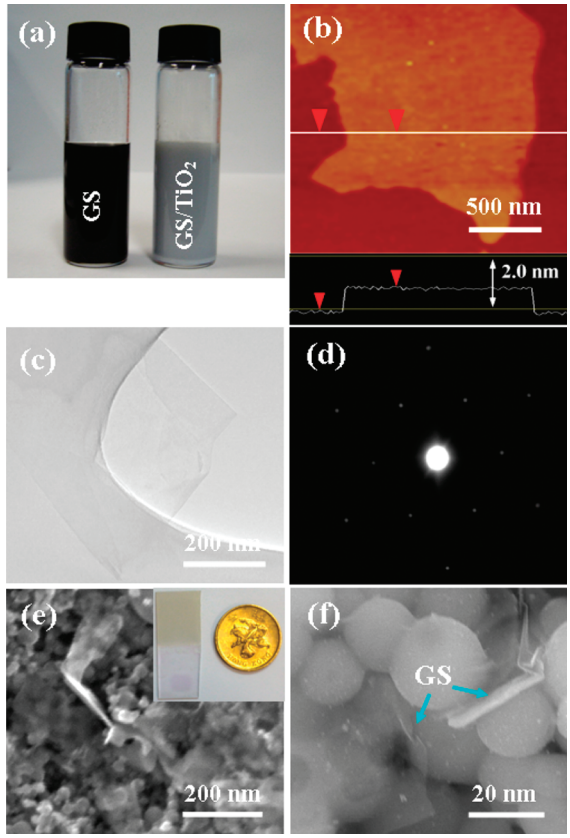

Figure 2. (a) Photographs of an ethanol dispersion with reduced graphene of sample 2 (left, 0.03 mg/mL) and GS/TiO_2 colloid suspension (right). (b) AFM image of a monolayer GS in sample 2 with a thickness of ~1.0 nm. (c) TEM image of a typical GS of sample 2, and (d) the corresponding electron diffraction (ED) pattern. (e,f) SEM images of the composite films deposited from the suspension with 0.03 mg/mL GS concentration. Inset in (e) is a photograph of the GS/TiO_2 film on ITO glass. The coin diameter is ~22 mm.

that the conductivity of reduced GS decreased with increasing oxidation time during the chemical exfoliation process. According to X-ray photoemission spectroscopy (XPS) analyses (Figure S3), such conductivity reduction is attributed to increase of residual oxygen-containing groups by increasing oxidation time. Therefore, controlling the oxidation time is important to optimize the conductivity of the reduced GS prepared by the chemical exfoliation method.

Owing to the presence of residual oxygen-containing functional groups,[12,13] such as hydroxyl, titanium alkoxide (titanium(IV) butoxide in this study) can be readily grafted on the reduced GS surfaces by chemisorption at the molecular level (Figure 1b). Additional sonication assists dispersion of the titanium alkoxide among the GS suspension and promotes the reaction between the titanium precursor and the functional groups on the GS surfaces. Once aqueous solution was added dropwise to the suspension under vigorous stirring, GS/TiO_2 colloids were formed *via* hydrolysis reaction between the adsorbed alkoxide and water molecules (Figure 1c). Note that the hydrolysis of adsorbed alkoxide supplies hydroxyl groups again to the colloid surfaces. Therefore, 1 M HNO_3 (2.0 mL) as charger was then added to render the composite colloids positively charged. The resulting suspension was gray and found to be stable for several weeks without phase separation (Figure 2a, left), indicating a uniform dispersion of positive-charged GS/TiO_2 colloids. It was revealed that attachment of TiO_2 nanoparticles to GS is not significant in sample 1 (Supporting Information, Figure S4a,b) with only 5 h oxidation time, whereas the attachment of TiO_2 nanoparticles is considerable in samples 2 and 3 with oxidation times longer than 10 h (Figure S4c,d). Combining this with the XPS results (Figure S3), we deduce that the good attachment of TiO_2 nanoparticles in samples 2 and 3 is due to the increase of residual oxygen-containing groups on the reduced GS for the long oxidation process.

Synthesis of GS/TiO_2 Composite Films. In this case, the GS/TiO_2 colloid suspension of sample 2 was utilized to prepare GS/TiO_2 composite films due to its sufficient attachment of TiO_2 nanoparticles and high conductivity of reduced GS. GS/TiO_2 composite films on conductive glass for PV applications were prepared by electrophoretic deposition (Figure 1d). Briefly, a graphite plate and a piece of indium tin oxide (ITO)-coated glass were used as the positive and negative electrodes, respectively. Under an applied voltage, the positively charged GS/TiO_2 colloids migrated toward the negative electrode and were deposited orderly onto the ITO-coated glass. Generally, the thickness of the composite films depends on the deposition time at a constant voltage. For a deposition time of 3 min at 30 V, the film thickness is about 460 nm, which was estimated from the interference oscillations in the UV−visible spectra. These films were rinsed with deionized water and calcined in vacuum to improve crystallinity of the TiO_2 nanoparticles.

The composite films synthesized by this method were macroscopically uniform and had large areas up to centimeter scale, limited only by the size of the substrate (inset in Figure 2e). It was also observed that the process is highly reproducible, giving composite films with consistent properties throughout batches. Figure 2e shows a typical scanning electron microscopy (SEM) image of the composite film. The GS in the composite films can be observed more clearly from a high-magnification SEM image (Figure 2f).

Conductivity Measurement of GS/TiO_2 Composite Films. The incorporation of GS into the TiO_2 nanoparticle film significantly improves the film conductivity. Figure 3a depicts an $I-V$ curve for a composite film (~460 nm thick) deposited from the colloid suspension with a GS concentration of 0.03 mg/mL (the deposition duration was 3 min). As a control, we fabricated a TiO_2 film by the same process without adding GS; the $I-V$ curve is also shown in Figure 3a. For the control sample, very little current (on the order of pA) passes through the film between two silver (1 × 1 mm) electrodes 1 mm apart.

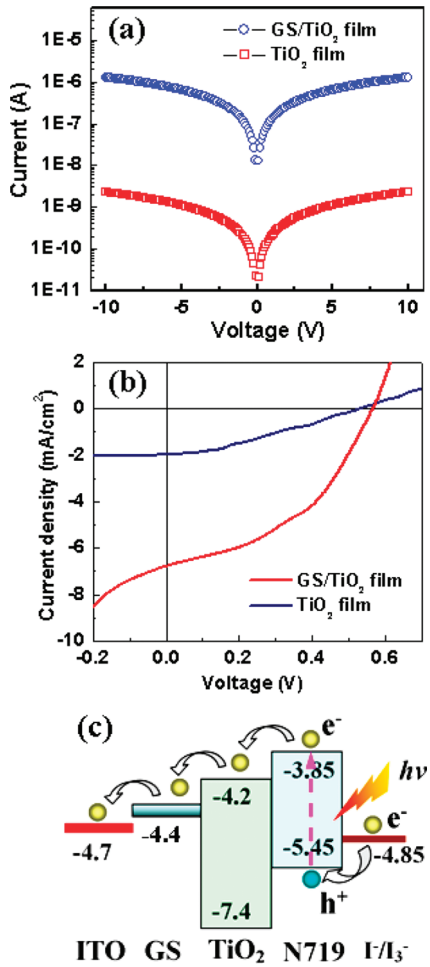

Figure 3. (a) Semilogarithmic current−voltage (*I*−*V*) curves of the GS/TiO_2 film (~460 nm thick) prepared from the suspension with a GS concentration of 0.03 mg/mL and the pure TiO_2 film. (b) Current density−voltage (*J*−*V*) characteristics of DSSCs based on GS/TiO_2 and TiO_2 nanoparticle films under 1 sun illumination. (c) Schematic energy-level diagram for the GS/TiO_2 DSSC.

However, incorporation of GS into the film dramatically increases the current to the level of μA. The calculated resistivity decreased by more than 2 orders of magnitude from $2.1 \pm 0.9 \times 10^5\ \Omega \cdot$cm (close to that of intrinsic TiO_2 films)[27] for the control sample to $3.6 \pm 1.1 \times 10^2\ \Omega \cdot$cm for the GS/$TiO_2$ composite film due to the high conductivity of reduced GS (Supporting Information, Figure S2).

GS/TiO_2 Dye-Sensitized Solar Cells. Using the composite films as the photoanode, we fabricated DSSCs to evaluate the PV performances. PV test for all cells with an active cell area of 0.5×0.5 cm^2 was carried out under AM 1.5G simulated sunlight with an intensity of 100 mW/cm^2 (equivalent to 1 sun). Figure 3b shows the current density−voltage (*J*−*V*) characteristics of the cells with and without GS. Under simulated illumination, the cell based on GS/TiO_2 film gave a short-circuit current density (J_{SC}) of 6.67 mA/cm^2, an open-circuit voltage (V_{OC}) of 0.56 V, and a fill factor (FF) of 0.45, yielding a power conversion efficiency (η) of 1.68%. For the control cell fabricated by the same process without adding GS, the corresponding values were $J_{SC} = 1.95$ mA/cm^2, $V_{OC} = 0.52$ V, FF = 0.31, and $\eta = 0.32\%$. Comparing the PV performances of the two cells, it is clear that, while the V_{OC} is similar, there is a significant improvement in both J_{SC} and FF for the cell based on GS/TiO_2, leading to about 5-fold increase in the power conversion efficiency. According to previous reports,[23,24] the improvement in the overall PV performance (mainly due to the increase in J_{SC}) for the GS/TiO_2 cell should be attributed to the decreased charge-transfer resistance in the composite films as a result of the implanted GS, which creates a continuous electron conducting network to the transparent electrode, facilitating the transport of photoinjected electrons and lowering probability of recombination.[23,24]

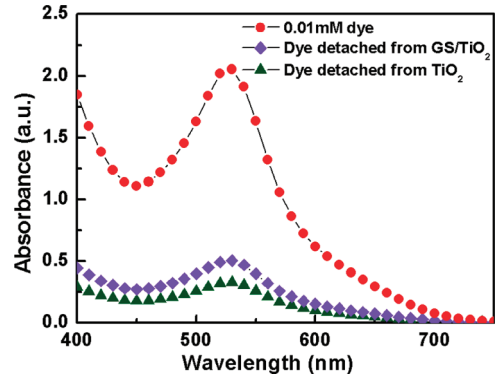

Figure 4. Absorptions of solutions containing 0.01 mM dye and dyes detached from the GS/TiO_2 and TiO_2 films.

Mechanism of Improved PV Performance. The transport mechanism of the GS/TiO_2 composite cell can be understood from an energy-level diagram. The work function of the reduced GS films was determined by ultraviolet photoemission spectroscopy (UPS) to be ~4.4 eV (Supporting Information, Figure S5). The schematic energy-level diagram for the GS/TiO_2 cell is depicted in Figure 3c. It can be seen that the offset (~0.2 eV) between the conduction band minimum of TiO_2 and the work function of graphene is sufficient for charge separation. Meanwhile, the GS will not block the injected electrons flowing down to the transparent electrode because its work function is higher than that of the ITO electrode. Therefore, the implanted graphene sheets serve as the electron acceptor and transporter for effective charge separation and rapid transport of the photogenerated electrons.[23,24] In addition, a previous report confirmed that GS could improve the adsorptivity of dyes in the GS/TiO_2 system.[24] We carried out dye desorption experiments to verify the difference of dye loading between GS/TiO_2 and TiO_2 films. Figure 4 shows the absorptions of solutions containing 0.01 mM dye and dyes detached from the GS/TiO_2 and TiO_2 films (both with 1 cm^2 area) in 10 mL of H_2O with 0.1 mM KOH. Using the 0.01 mM dye solution as the reference, we can calculate the dye loadings of GS/TiO_2 and TiO_2

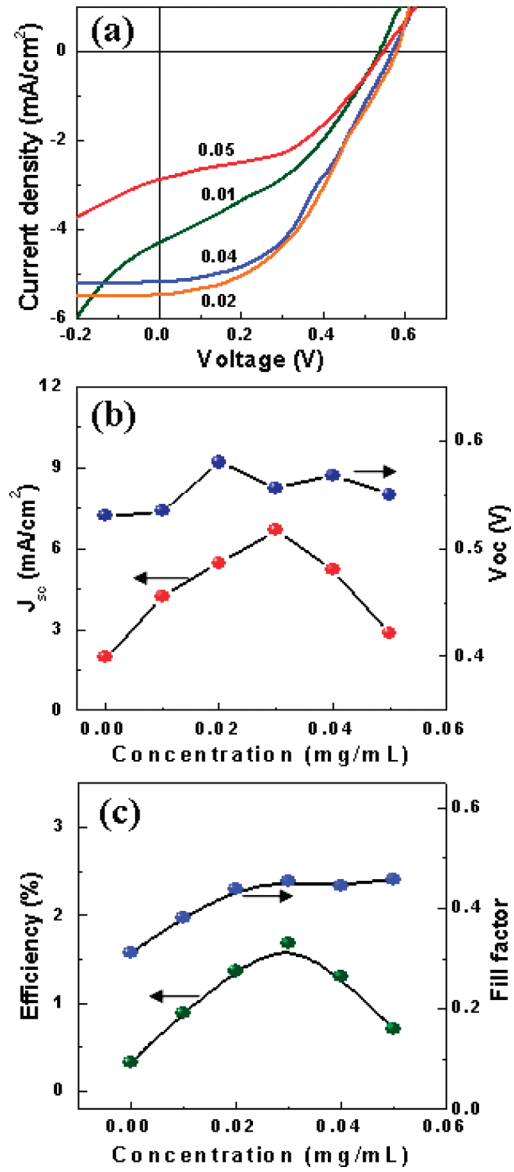

Figure 5. (a) *J*−*V* characteristics for DSSCs prepared with different GS concentrations (0.01, 0.02, 0.04, and 0.05 mg/mL) under 1 sun intensity. (b,c) Short-circuit current density (J_{SC}), open-circuit voltage (V_{OC}), fill factor (FF), and power conversion efficiency (η) of DSSCs with varying GS concentration.

films as ~1.6 × 10^{-6} and ~2.5 × 10^{-6} mol/cm^2, respectively. Although both films have relatively low dye loading, the GS/TiO_2 film exhibits remarkable improvement in dye loading compared to the TiO_2 film. Therefore, better dye loading also contributes to the better performance of GS/TiO_2 DSSC.

Effect of GS Concentration on the PV Performance. Figure 5a−c shows the *J*−*V* curves and the variation of the PV characteristics of the cells prepared from mixed solutions with different graphene concentrations (0.01−0.05 mg/mL). It can be seen that the J_{SC} first increased with increasing GS concentration, reaching a peak value of 6.67 mA/cm^2 at a GS concentration of 0.03 mg/mL, and then declined to 2.85 mA/cm^2 at 0.05 mg/mL. However, the V_{OC} values remained fairly constant in the range of 0.5−0.6 V. Unlike J_{SC}, V_{OC} is determined by the difference between the redox potential of the electrolyte and the Fermi level of TiO_2 rather than the device structure.[25] The initial increase and later decrease of J_{SC} can be explained by the increased conductivity according to the resistivity measurements (Supporting Information, Figure S7). As the GS concentration increases, say to 0.03 mg/mL, the formation of more conductive pathways by GS significantly decreases the transport resistance for photogenerated electrons and thus increases the photocurrent. On the other hand, increase of GS concentration also led to a decrease of the transmittance of visible light through the composite films (Figure S8), also reported previously,[11] in which the transmittance of GS films decreased with increasing film thickness. Consequently, the enhanced conductivity is offset by the decreased transmittance, which accounts for the decrease of J_{SC} at higher GS concentration. Similar to the trend of J_{SC}, the overall efficiency increases first, reaching a peak value of 1.68% at 0.03 mg/mL GS concentration, and then decreases (Figure 5c). Note that the relatively low efficiency in our cells at present is probably due to the low dye loading due to the small thickness (~0.5 μm) of the composite films. In conventional DSSCs,[15] the thickness of TiO_2 nanoparticles is typically >10 μm for anchoring a large amount of dye molecules. Improvement of the PV performances can be expected *via* substantially optimizing device structures, such as increasing the thickness of the composite films to increase dye loading or processing *via* the $TiCl_4$ treatment.[28]

CONCLUSIONS

We have demonstrated a simple and effective method to incorporate graphene sheets in TiO_2 nanoparticle films *via* molecular grafting, which consists of attaching titanium alkoxide onto functionalized graphene sheets by chemisorption. It was found that controlling the oxidation time is important to achieve both high conductivity of reduced GS and good attachment of TiO_2 nanoparticles on the GS. Large-area GS/TiO_2 composite films deposited on ITO glass exhibited much higher conductivity than the TiO_2 matrix films. In addition, the GS/TiO_2 films exhibit significant improvement in dye loading compared to the TiO_2 films. Composite films prepared from various GS concentrations were employed as the photoanode for DSSCs. The implanted GS provides transport pathways for the photogenerated carriers and significantly increases photocurrent through DSSCs. The maximum power conversion efficiency for DSSC based on the GS/TiO_2 nanocomposite was more than 5 times higher than that based on TiO_2 alone, which shows that incorporation of GS is an efficient means for enhancing the PV performance of TiO_2-based DSSCs. Further improvements can be expected by optimizing fabrication conditions and de-

vice configuration, as well as increasing dye loading *via* thicker films or by $TiCl_4$ treatment. The present synthetic strategy is expected to lead to a family of composites with designed properties.

EXPERIMENTAL SECTION

Functionalized GS suspension was synthesized by chemical reduction of exfoliated graphite oxide, which was prepared *via* a modified Hummers method,[25] starting from graphite flakes of ~20 μm size (Sigma Aldrich). First, three mixtures of graphite (2 g), $KMnO_4$ (10 g), concentrated HNO_3 (20 mL), and concentrated H_2SO_4 (60 mL) were vigorously stirred for 5, 10, and 20 h, and the samples are denoted as 1, 2, and 3, respectively. Afterward, the three samples were treated with 20 mL of H_2O_2 (30 wt %) for 2 days to complete the oxidation. Then, the mixtures were filtered through a 0.2 μm Nylon Millipore filter, washed with 3 wt % HCl, and deionized water to reduce residual ions and dried at 60 °C overnight. The obtained GO powders were rapidly heated at 1000 °C for 1 min and quickly cooled to room temperature under argon atmosphere. Exfoliation was carried out by sonicating thermal-expanded GO in purified water for 1 h. Afterward, GO suspensions were reduced by hydrazine (100 mL) for 24 h and centrifuged at 10 000 rpm for 10 min to form homogeneous GS dispersions, which was dried *via* evaporation of water at 60 °C. Finally, 20 mg of the as-prepared graphene sheets from each sample was washed copiously with ethanol and dispersed again in 200 mL of anhydrous ethanol by sonication for 1 h. Dispersions with various concentrations (0.01−0.05 mg/mL) were prepared by diluting a 0.1 mg/mL stock solution in ethanol.

For preparation of GS/TiO_2 composite colloids, 3 mL of titanium(IV) butoxide ($Ti[O(CH_2)_3CH_3]_4$, Aldrich) was dispersed in the 10 mL GS suspension (with GS concentration of 0.01−0.05 mg/mL) under sonication for 1 h. Organic titanium molecules can be readily grafted on the functionalized GS by chemisorption due to the presence of residual oxygen-containing functional groups.[2−4] Subsequently, 30 mL of deionized water was slowly added dropwise to the mixture with vigorous stirring, followed by 3 h sonication, after which the color of the suspension changed from black to gray. Note that the hydrolysis of adsorbed alkoxide supplies hydroxyl groups again on the colloid surfaces. Therefore, 1 M HNO_3 (2.0 mL) as charger was then added to render the GS/TiO_2 colloids positively charged. The final suspension was found to be stable for several weeks.

To investigate the conductivity of the reduced GS prepared by different oxidation times, we fabricated two-terminal devices based on individual graphene by dropping the GS suspension onto Si−SiO_2 substrates between a pair of parallel Au (~30 nm) electrodes spaced 2 μm. More than 10 devices were tested to confirm statistically the electrical output performance, with all measurements carried out at room temperature.

The GS/TiO_2 composite films on ITO glass for PV applications were prepared by electrophoretic deposition. Briefly, a graphite plate and a piece of ITO glass (~10 Ω/□) were used as the positive and negative electrodes, respectively. The distance between the two electrodes was 2−3 cm, and the applied voltage was 20−50 V. Under the applied voltage, the positively charged GS/TiO_2 colloids migrated toward the negative electrode and were deposited onto the ITO glass. For a deposition time of 3 min at 30 V, the thickness of the composite films was ~460 nm. These films were rinsed with deionized water and dried at 80 °C for 12 h, followed by calcination at 400 °C for 30 min in vacuum to improve the crystallization of TiO_2 nanoparticles.

For DSSC fabrication, the resulting films were sensitized by immersing in an ethanol solution containing 0.5 mM N719 dye (Solaronix Inc.) for 24 h. Afterward, the sensitized films were sandwiched and bonded with a platinum (~30 nm)-coated ITO counter electrode. The two electrodes were separated by a ~20 μm thick polypropylene spacer, and the internal space of the cells was filled with a liquid electrolyte (0.1 M LiI, 50 mM I_2, and 0.6 M DMPII (Solaronix)) in acetonitrile by capillary action. The active area of the DSSCs was 0.5 × 0.5 cm^2.

Acknowledgment. The authors thank Drs. T. F. Hung and Y. M. Chong for their kind help in TEM and AFM experiments. The work was supported by the Research Grants Council of Hong Kong (Grant No. CityU101809), a NSFC/RGC Joint Research Scheme (No. N_CityU108/08) of Research Grants Council of Hong Kong SAR, China, and the National 973 projects of the Major State Research Development Program of China (Grant Nos. 2006CB933000 and 2007CB936000), and the IMR SYNL-T.S. Kê Research Fellowship.

Supporting Information Available: More AFM characteristics of reduced GS, *I*−*V* measurements of the reduced GS prepared by different oxidation times, XPS spectra of GO precursors and reduced GS from samples 1−3, SEM images of the attachment of TiO_2 nanoparticles on graphene sheets, typical HeI UPS spectrum of the reduced graphene sheets, schematic structure of the DSSCs, resistivity of GS/TiO_2 films as a function of GS concentration, transmittance spectra, and photograph image of GS/TiO_2 films deposited from different GS concentrations. This material is available free of charge *via* the Internet at http://pubs.acs.org.

REFERENCES AND NOTES

1. Novoselov, K. S.; Geim, A. K.; Morozov, S. V.; Jiang, D.; Zhang, Y.; Dubonos, S. V.; Grigorieva, I. V.; Firsov, A. A. Electric Field Effect in Atomically Thin Carbon Films. *Science* **2004**, *306*, 666–669.
2. Geim, A. K.; Novoselov, K. S. The Rise of Graphene. *Nat. Mater.* **2007**, *6*, 183–191.
3. Novoselov, K. S.; Geim, A. K.; Morozov, S. V.; Jiang, D.; Katsnelson, M. I.; Grigorieva, I. V.; Dubonos, S. V.; Firsov, A. A. Two-Dimensional Gas of Massless Dirac Fermions in Graphene. *Nature* **2005**, *438*, 197–200.
4. Zhang, Y.; Tan, Y. W.; Stormer, H. L.; Kim, P. Experimental Observation of the Quantum Hall Effect and Berry's Phase in Graphene. *Nature* **2005**, *438*, 201–204.
5. Li, X. L.; Wang, X.; Zhang, L.; Lee, S.; Dai, H. J. Chemically Derived, Ultrasmooth Graphene Nanoribbon Semiconductors. *Science* **2008**, *319*, 1229–1232.
6. Li, X. L.; Zhang, G. Y.; Bai, X. D.; Sun, X. M.; Wang, X. R.; Wang, E. G.; Dai, H. J. Highly Conducting Graphene Sheets and Langmuir−Blodgett Films. *Nat. Nanotechnol.* **2008**, *3*, 538–542.
7. Tang, Y. B.; Lee, C. S.; Chen, Z. H.; Yuan, G. D.; Kang, Z. H.; Luo, L. B.; Song, H. S.; Liu, Y.; He, Z. B.; Zhang, W. J.; Bello, I.; Lee, S. T. High-Quality Graphenes *via* a Facile Quenching Method for Field-Effect Transistors. *Nano Lett.* **2009**, *9*, 1374–1377.
8. Gilje, S.; Song, H.; Wang, M.; Wang, K. L.; Kaner, R. B. A Chemical Route to Graphene for Device Applications. *Nano Lett.* **2007**, *7*, 3394–3398.
9. Eda, G.; Fanchini, G.; Chhowalla, M. Large-Area Ultrathin Films of Reduced Graphene Oxide as a Transparent and Flexible Electronic Material. *Nat. Nanotechnol.* **2008**, *3*, 270–274.
10. Schedin, F.; Geim, A. K.; Morozov, S. V.; Hill, E. W.; Blake, P.; Katsnelson, M. I.; Novoselov, K. S. Detection of Individual Gas Molecules Adsorbed on Graphene. *Nat. Mater.* **2007**, *6*, 652–655.
11. Wang, X.; Zhi, L.; Mullen, K. Transparent, Conductive Graphene Electrodes for Dye-Sensitized Solar Cells. *Nano Lett.* **2008**, *8*, 323–327.
12. Stankovich, S.; Dikin, D. A.; Dommett, G. H. B.; Kohlhaas, K. M.; Zimney, E. J.; Stach, E. A.; Piner, R. D.; Nguyen, S. T.; Ruoff, R. S. Graphene-Based Composite Materials. *Nature* **2006**, *442*, 282–286.
13. Watcharotone, S.; Dikin, D. A.; Stankovich, S.; Piner, R.; Jung, I.; Dommett, G. H. B.; Evmenenko, G.; Wu, S. E.; Chen,

S. F.; Liu, C. P.; Nguyen, S. T.; Ruoff, R. S. Graphene−Silica Composite Thin Films as Transparent Conductors. *Nano Lett.* **2007**, *7*, 1888–1892.
14. Eda, G.; Chhowalla, M. Graphene-Based Composite Thin Films for Electronics. *Nano Lett.* **2009**, *9*, 814–818.
15. Regan, B. O.; Gratzel, M. A. Low-Cost, High-Efficiency Solar-Cell Based on Dye-Sensitized Colloidal TiO_2 Films. *Nature* **1991**, *353*, 737–740.
16. van de Lagemaat, J.; Benkstein, K. D.; Frank, A. J. Relation between Particle Coordination Number and Porosity in Nanoparticle Films: Implications to Dye-Sensitized Solar Cells. *J. Phys. Chem. B* **2001**, *105*, 12433–12436.
17. Kopidakis, N.; Neale, N. R.; Zhu, K.; van de Lagemaat, J.; Frank, A. J. Spatial Location of Transport-Limiting Traps in TiO_2 Nanoparticle Films in Dye-Sensitized Solar Cells. *Appl. Phys. Lett.* **2005**, *87*, 202106.
18. Du, P. A.; Chen, H. H.; Lu, Y. C. Dye Sensitized Solar Cells Using Well-Aligned Zinc Oxide Nanotip Arrays. *Appl. Phys. Lett.* **2006**, *89*, 253513.
19. Law, M.; Greene, L. E.; Johnson, J. C.; Saykally, R.; Yang, P. D. Nanowire Dye-Sensitized Solar Cells. *Nat. Mater.* **2005**, *4*, 455–459.
20. Kongkanand, A.; Kamat, P. V. Electron Storage in Single Wall Carbon Nanotubes. Fermi Level Equilibration in Semiconductor−SWCNT Suspensions. *ACS Nano* **2007**, *1*, 13–21.
21. Kongkanand, A.; Dominguez, P. M.; Kamat, P. V. Single Wall Carbon Nanotube Scaffolds for Photoelectrochemical Solar Ccells. Capture and Transport of Photogenerated Electrons. *Nano Lett.* **2007**, *7*, 676–680.
22. Williams, G.; Seger, B.; Kamat, P. TiO_2−Graphene Nanocomposites. UV-Assisted Photocatalytic Reduction of Graphene Oxide. *ACS Nano* **2008**, *2*, 1487–1491.
23. Manga, K. K.; Zhou, Y.; Yan, Y. L.; Loh, K. P. Multilayer Hybrid Films Consisting of Alternating Graphene and Titania Nanosheets with Ultrafast Electron Transfer and Photoconversion Properties. *Adv. Funct. Mater.* **2009**, *19*, 3638–3643.
24. Zhang, H.; Lv, X. J.; Li, Y. M.; Wang, Y.; Li, J. H. P25-Graphene Composite as a High Performance Photocatalyst. *ACS Nano* **2009**, *4*, 380–386.
25. Hummers, W. S.; Offeman, J. R. E. Preparation of Graphitic Oxide. *J. Am. Chem. Soc.* **1958**, *80*, 1339.
26. Stankovich, S.; Dikin, D. A.; Piner, R. D.; Kohlhaas, K. A.; Kleinhammes, A.; Jia, Y.; Wu, Y.; Nguyen, S. T.; Ruoff, R. S. Synthesis of Graphene-Based Nanosheets *via* Chemical Reduction of Exfoliated Graphite Oxide. *Carbon* **2007**, *45*, 1558–1565.
27. Neumann, E.; Bierau, F.; Johnson, B.; Kaufmann, C. A.; Ellmer, K.; Tributsch, H. Niobium-Doped TiO_2 Films as Window Layer for Chalcopyrite Solar Cells. *Phys. Status Solidi (b)* **2008**, *245*, 1849–1857.
28. Peter, L. M. Dye-Sensitized Nanocrystalline Solar Cells. *Phys. Chem. Chem. Phys.* **2007**, *9*, 2630–2642.